ARTICLE
Journal of Cellular Biochemistry 111:1473–1481 (2010)

Journal of Cellular Biochemistry

Effect of Cleidocranial Dysplasia-Related Novel Mutation of RUNX2 on Characteristics of Dental Pulp Cells and Tooth Development

DongYing Xuan,[1] Xi Sun,[1] YuXia Yan,[2] BaoYi Xie,[1] PingPing Xu,[1] and JinCai Zhang[1*]

[1]*Department of Periodontology, Guangdong Provincial Stomatological Hospital, Southern Medical University, Guangzhou, China*

[2]*Department of Biostatistics, School of Public Health and Tropical Medicine, Southern Medical University, Guangzhou, China*

ABSTRACT

Cleidocranial dysplasia (CCD) is an autosomal-dominant disorder caused by a lack of function of one or more alleles of the *RUNX2* gene. Mutations of the *RUNX2* gene were analyzed in a family with CCD, and a novel nonsense mutation was identified, c. 1096G > T, p.E366X, which was predicted to cause a number of potential dysfunctions. Western blot analysis showed that the novel mutation created a shortened protein product, which lost 155 aa in the C-terminal domain. The mutant protein was detected to be localized mostly in the cytoplasm, not in the nucleus, which demonstrated that transport of the RUNX2 protein into the nucleus was disturbed by the p.E366X mutation. For the first time, $RUNX2^{+/m}$ dental pulp cells (DPCs) were isolated from two permanent incisors of the CCD patient. Compared to $RUNX2^{+/+}$ controls, $RUNX2^{+/m}$ DPCs presented an impeded progression from the G1 to the S phase in the cell cycle, a lower rate of proliferation, weaker ability of calcification, and distinct ultrastructure. More interestingly, the ultrastructural analysis and energy dispersive X-ray spectrometry (EDS) analysis showed that the CCD tooth exhibited insufficient mineralization of enamel and dentin. This study suggests that the truncated RUNX2 mutant protein may be responsible for the alterations of $RUNX2^{+/m}$ DPCs, and *RUNX2* gene may be involved in dental development by affecting the cell growth and differentiation, which provides new insights into understanding of dental abnormalities in CCD patients. J. Cell. Biochem. 111: 1473–1481, 2010.

KEY WORDS: CLEIDOCRANIAL DYSPLASIA; *RUNX2* GENE; MUTATION; DENTAL PULP CELL

Cleidocranial dysplasia (CCD) is an autosomal-dominant disorder caused by a lack of function of one or more alleles of the *RUNX2* gene (previously named *CBFA1*) [Mundlos et al., 1997]. The primary symptoms of CCD include open fontanelles, hypoplasia or aplasia of the clavicles, a wide pubic symphysis, and short stature. This disorder is often accompanied by dental abnormalities including supernumerary teeth, abnormal tooth eruption, tooth hypoplasia and lack of cellular cementum formation [Mundlos, 1999]. Runx2 is a transcription factor that is necessary for osteoblast and dental cell differentiation as well as bone and tooth formation [Ducy et al., 1997].

In addition to being a key player in osteoblast lineage determination, differentiation pathways and bone formation, studies have shown that *Runx2* regulates genes related to cell growth and controls osteoblast proliferation. Mice with a targeted disruption of $Runx2^{-/-}$ show no osteoblast differentiation and a complete disruption of bone formation, and they also exhibit dysfunctions in early dental development. Tooth germs are arrested at the cap/early bell stages with no odontoblast cytodifferentiation or dentin formation [D'Souza et al., 1999]. *Runx2* controls the transcription of many bone- and tooth-related genes through its DNA binding site. *Runx2* is regulated by bone morphogenetic proteins (BMPs), the transforming growth factor β (TGF-β) family, and signal transducer Smad proteins [Zhang et al., 2000; Aberg et al., 2004].

Differential expression of Runx2 isoforms (type I–II) has been demonstrated in odontoblast and dental pulp cells (DPCs) during tooth development in mice [Chen et al., 2002]. Several in vivo and in

Xuan Dongying and Sun Xi contributed equally to this work.

Grant sponsor: National Natural Science Foundation of China; Grant number: 30901691; Grant sponsor: Medical Scientific Research Fund of Guangdong Province; Grant number: B2008015.

*Correspondence to: Jincai Zhang, Department of Periodontology, Guangdong Provincial Stomatological Hospital, Southern Medical University, S366 Jiangnan Boulivard, Guangzhou 510280, China. E-mail: xuanxuan187@126.com

Received 29 July 2010; Accepted 1 September 2010 • DOI 10.1002/jcb.22875 • © 2010 Wiley-Liss, Inc.
Published online 24 September 2010 in Wiley Online Library (wileyonlinelibrary.com).

vitro studies have demonstrated that DPCs are capable of differentiating into odontoblasts and producing a mineralizing matrix, particularly during reparative dentinogenesis [Goldberg and Lasfargues, 1995]. Runx2 is essential for osteoblast differentiation; however, it remains unknown whether Runx2 plays a key role in DPCs differentiation. Although human primary DPCs were established from a CCD patient, and cell morphology and growth rate were initially investigated [Chen et al., 2005], the characteristics of human DPCs from permanent teeth have never been explored.

In the present study, a novel nonsense mutation was identified in two patients with CCD, which resulted in a shortened protein product. For the first time, human DPCs were established from permanent teeth of a CCD patient, and the biological characteristics are investigated initially. The ultrastructural analysis indicated poor mineralization of the CCD teeth. Our data presented herein provide new insights regarding the potential role of *RUNX2* gene in tooth development and dental abnormalities of CCD patients.

MATERIALS AND METHODS

CASE REPORT

Patient 1 was a 28-year-old female, who was initially referred at age 15 with dysmorphia and short stature. Patient 2 was the 23-year-old brother of patient 1, who was initially referred at age 13 with dental abnormalities and an open fontanel. A CCD phenotype was confirmed by the presence of hypoplastic clavicles, delayed closure of the anterior fontanel, as well as typical craniofacial features [for review of diagnostic criteria, see Mundlos, 1999]. The two sibling patients, the youngest brother, and their parents were investigated. Blood samples were obtained from all the families except for the mother who refused. Radiological examinations for osseous malformations were carried out for each individual (including the mother). This study was approved by the Ethics Committee of Southern Medical University, and informed consent was obtained from all individuals.

MUTATION ANALYSIS OF *RUNX2* GENE

DNA was extracted from blood samples with the QIAamp Blood Kit (Qiagen). Exons 0–7 of the *RUNX2* gene were amplified from genomic DNA and sequenced as previously outlined [Xuan et al., 2008]. Briefly, the PCR reaction was performed with a 5 min denaturation at 94°C, followed by 25 cycles, each with denaturation at 94°C for 30 s, primer annealing for 30 s at different temperature respectively (Table I), and product extension at 72°C for 1 min. DNA sequences were analyzed using BLASTN (BLAST nucleotide) program (http://www.ncbi.nlm.nlh.gov/BLAST). After a mutation within exon 7 was detected in the patients, exon 7 was amplified and sequenced from the father, the youngest brother and 100 unrelated normal people, as outlined above.

IDENTIFICATION OF DENTAL PULP CELLS FROM A CCD PATIENT

DPCs were isolated from two extracted permanent incisors of CCD patient 1 (for restoration of occlusion and prosthetics), as well as from a normal age- and sex-matched control individual. The pulp was separated and digested with a solution of 3 mg/ml collagenase type I and 4 mg/ml dispase for 1 h at 37°C. Pulp explants were grown in alpha minimal essential medium (a-MEM), supplemented with 10% fetal calf serum and 100 units/ml of penicillin/streptomycin. The cultures were examined routinely utilizing an inverted microscope (Olympus, Japan). The cells from patient 1 were named *RUNX2*$^{+/m}$ *DPCs*, and the cells from control individual were named *RUNX2*$^{+/+}$ *DPCs*. Cells between the third and fifth passages were used for analysis.

Expression of *RUNX2* gene was examined in DPCs by reverse transcription polymerase chain reaction (RT-PCR). Total RNAs from DPCs were isolated and reverse-transcribed using the SMART^{TM} PCR cDNA synthesis kit. Primers specific for *RUNX2* gene (P1 and P2) were used. Primers P1 (5′-CGG CCG CCC CAC GAC AAC C-3′, upstream) and P2 (5′-GGC GGG ACA CCT ACT CTC ATA CTG-3′, downstream) yielded an amplicon of 504 bp. A 20 μl volume of reverse-transcribed product was amplified with Taq DNA polymerase. The reaction was performed with a 5-min denaturation at 94°C, followed by 30 cycles each with denaturation at 94°C for 50 s, primer annealing at 58°C for 30 s, and product extension at 72°C for 1 min.

EXPRESSION ANALYSIS OF MUTANTS RUNX2 PROTEIN IN DPCS

To detect the expression of RUNX2 mutants, Western blotting was performed to analyze the extracts of *RUNX2*$^{+/m}$ and *RUNX2*$^{+/+}$ DPCs. The 5×10^6 cells at the 3rd passage (P3) were prepared in the lysis buffer (according to the proportion of 0.5 g sample in 1 ml lysis buffer). After quantitation of the collected total proteins, 10 μg protein from each sample was separated on 12% denaturing gels, transferred onto a polyvinylidene fluoride membrane. The membrane was then blocked with 5% fat free dry milk for 2 h at room temperature, and incubated at 4°C overnight with primary antibody against RUNX2 protein (mouse monoclonal antibody anti-RUNX2, 1:500 dilution, #D130-3, MBL Co). The membrane was washed with TBST buffer and incubated with the corresponding secondary antibodies (rabbit anti-mouse immunoglobulins/HRP, 1:10,000 dilution, Dako). The membrane was washed for three times, and chemiluminescent HRP substrates were added on it for 5 min, and exposure was done in darkroom.

To evaluate the effect of the mutation on nuclear localization of RUNX2 protein, the immunocytochemistry analysis was done in *RUNX2*$^{+/m}$ and *RUNX2*$^{+/+}$ DPCs. The primary antibody was the same as used in western blotting (the dilution was changed as 1:100). Immunofluorescence labeling was performed with secondary antibody anti-mouse IgG-594 (1:300 dilution, Sigma) conjugated with fluorescein isothiocyanate (FITC). The cells were visualized and photographed with a fluorescent microscope (DMI6000B, Leica).

CHARACTERISTIC ANALYSIS OF RUNX2$^{+/M}$ DPCS

The two cell groups were cultured, respectively, with the same media under the same conditions as stated above. To measure the cell size, the two cell populations were observed and pictured with an inverted light microscope (Olympus), and the cell area was measured by Image-Pro Express version 6.0 (IPE 6.0) software (Olympus Sales & Service Co., Ltd., Guangzhou Branch). Six cells per visual field were randomly chosen and assayed, and five fields were observed, thus 30 cells in each group were measured.

Cell growth was assayed using a Coulter Counter according to the method proposed by Freshney [2001]. Briefly, cells at P3 were seeded in 24-well plates at 0.6×10^4 cells/plate, and the cells of three

TABLE I. Primers Used for the Polymerase Chain Reaction and Sequencing Reaction of *RUNX2* Gene

RUNX2	Sequence (5′–3′)	Annealing temperature (°C)	Product size (bp)
Exon 0	Forward TACCCAGCCACCGAGACCAACAGAG Reverse GTTTTGCTGACATGGTGTCAC	62	339
Exon 1	Forward ACTTGTGGCTGTTGTGATGC Reverse GCCGCCAAGGCAGGA	57	514
Exon 2	Forward CAGATGCTTGATTCCTGTCGG Reverse GTGCTGATTTGTATACAGACTAG	62	391
Exon 3	Forward TCATTGCCTCCTTAGAGATGC Reverse GGACATGAAAGTGACACTAAC	62	310
Exon 4	Forward TATAAAGCAATTTGAAATGCAAGG Reverse GTTTTGAAGTGAACACATCTCC	57	428
Exon 5	Forward TAAGGCTGCAATGGTTGCTAT Reverse GTCACTGTGAGCATGGATGAG	62	306
Exon 6	Forward TAGAACATTAGAGCTGGAAGG Reverse CGGACAGTAACAACCAGACAG	62	189
Exon 7	Forward TGTGGCTTGCTGTTCTTTATG Reverse GATACCACTGGGCCACTGCT	62	630

wells were counted daily. This experiment was performed repeatedly three times.

Flow cytometric analysis was performed to assay the cell cycle by flow cytometer (Beckman Coulter, Elite). Cells (1×10^6) at P3 were collected and centrifuged for 5 min at 1,000 rpm, and the deposition was washed with 0.1 M phosphate buffer (pH 7.4, PBS) twice, then fixed with pre-cooling ethanol for 20 min, and dyed with propidium iodide (PI, 50 μg/ml, Sigma) for 30 min in the dark area. Finally, the cell suspension was detected by flow cytometer.

Ultrastructure of the cells was observed with a transmission electron microscope (TEM, Philip CM10, Netherlands). Cells at P3 were scraped and centrifuged for 10 min at 1,000 rpm, and the deposition was collected and pre-fixed in 2.5% glutaraldehyde for 2 h, and washed with 0.1 M PBS (pH 7.2) for 15 min. Then the samples were post-fixed in 1% osmium tetroxide for 2 h, washed with PBS for 15 min, immersed in a graded ethanol series and followed by pure acetone and acetone-epoxy series, then embedded in epoxy resin. Fifty to 60 nm sections were cut, and the sections on the grids were stained with 2% uranyl acetate and lead citrate. And the sections were examined on a TEM (Philip CM10).

CALCIFICATION INDUCTION

To detect the calcification potential of the *RUNX2*$^{+/m}$ DPCs, the Cells at P4 were seeded in 6-well plates at 0.3×10^5 cells/plate. When the cells grew and reached 80% confluence, the medium was changed as the a-MEM supplemented with 50 μg/ml ascorbic acid and 10 mM Na β-glycerophosphate (Sigma). After 5 weeks, the calcification ability of the cells was assayed by von Kossa staining. After fixation with 2% glutaraldehyde solution, the cultures were incubated with 5% $AgNO_3$ solution for 30 min in the dark. The staining was revealed by ultraviolet exposition for 1 h. The cultures were counterstained with Nuclear Fast Red. Secreted calcified extracellular matrix was observed as black nodules.

ULTRASTRUCTURE EXAMINATION AND ELEMENT ANALYSIS OF CCD TEETH

After the pulp was separated for DPC culture, the crown and root were examined without decalcification utilizing scanning electron microscopy (SEM). Sections were cut with a diamond blade and polished, then treated with 40% phosphoric acid for 10 s, washed with distilled water, dried in air, sputter-coated with gold, and mounted on aluminum stubs for viewing and photographing by SEM (FEI Quanta 400 SEM, Netherlands) at 25 kV. Three fields were randomly chosen in each dentin surface, and the elements (including calcium, phosphorus, carbon, oxygen, and chloride) were simultaneously analyzed using energy dispersive X-ray spectrometry (EDS, FEI Quanta 400) which was on-line connected with SEM. Briefly, when a field was chosen and analyzed automatically with EDS, the weight percentages of different elements were presented immediately. The percentage of chloride element was so small that it was omitted in the analysis.

DATA ANALYSIS

Statistical analyses were performed using the statistical software SPSS 13.0. The two comparisons were performed using two-tailed *t*-test, and the results are expressed as the means ± SE of at least three independent experiments. A *P*-value ≤ 0.05 was considered significant.

RESULTS

IDENTIFICATION OF A NOVEL NONSENSE MUTATION P.E366X

The clinical examination showed that the patient's youngest brother and parents were healthy, and patient 1 and patient 2 presented typical characteristics of CCD, such as hypoplastic clavicles, delayed closure of the anterior fontanel in addition to classic craniofacial features. Clinical characteristics of patient 1 and patient 2 were shown in Figures 1 and 2, respectively. Patient 1 presented retention of deciduous teeth, impacted and supernumerary teeth, and many of his teeth exhibited enamel exfoliation and dentin dysplasia.

To identify mutations of the *RUNX2* gene, the genomic DNAs were analyzed from the two patients, their healthy brother and father, and 100 unrelated healthy people. A novel nonsense mutation (c. 1096G > T, p.E366X) was identified in exon 7 of the both patients, while their father, the youngest brother, and all other healthy individuals did not carry the same mutation (Fig. 3A). The c. 1096G > T mutation converts the code GAA to TAA which is a termination code, therefore the mutation is predicted to yield a truncated protein lacking the C-terminal 155 amino acids (henceforth referred to as CCD E366X, Fig. 3B).

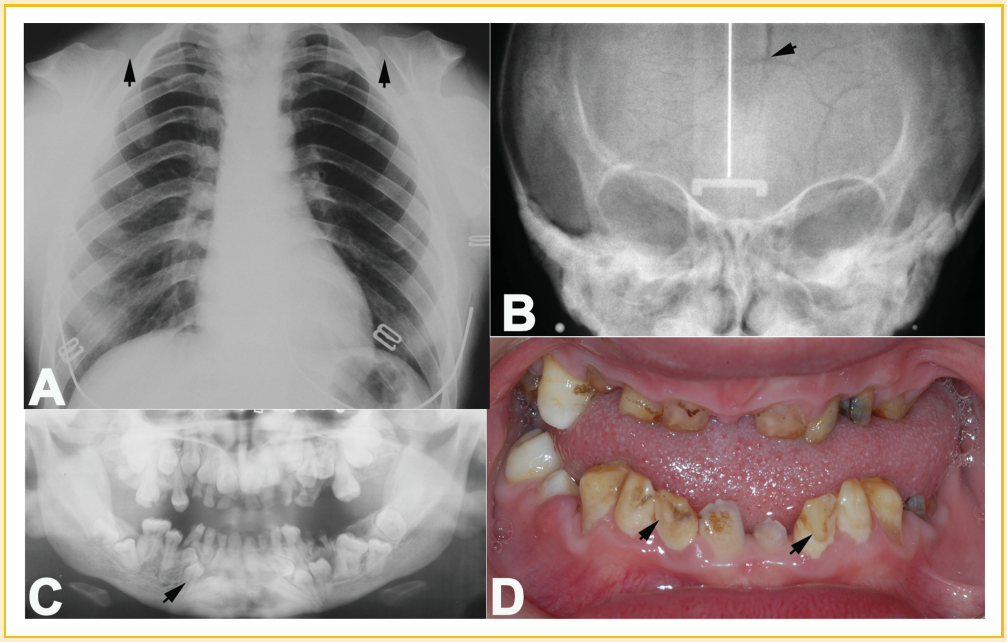

Fig. 1. Typical radiological and clinical morphologies from patient 1. A: Chest radiograph showing absent clavicle on the left and hypoplasia on the right clavicle. B: Posteroanterior cephalometric radiograph showing open sutures and fontanelle. C: Panoramic view showing imbedded permanent teeth and supernumerary teeth, and retention of deciduous teeth. D: Intraoral image showing enamel and dentin hypoplasia.

THE EFFECT OF THE TRUNCATED E366X MUTANT PROTEIN ON *RUNX2*$^{+/M}$ DPCS

RUNX2 gene expressed transcriptionally both in *RUNX2*$^{+/+}$ and *RUNX2*$^{+/m}$ DPCs (data were not shown). Western blotting analysis showed that the full-length RUNX2 protein presented in both of the two DPC groups, however, the mutant truncated CCD E366X was detected only in *RUNX2*$^{+/m}$ DPCs (Fig. 4A,B). According to the results of immunocytochemistry analysis, almost all the cells in the RUNX2$^{+/+}$ group had RUNX2 protein localized in the nucleus, not in the cytoplasm (Fig. 4C–E); however, for the *RUNX2*$^{+/m}$ DPCs, RUNX2 protein localized mostly in the cytoplasm, and a few cells had the protein both in the nucleus and in the cytoplasm (Fig. 4F–H).

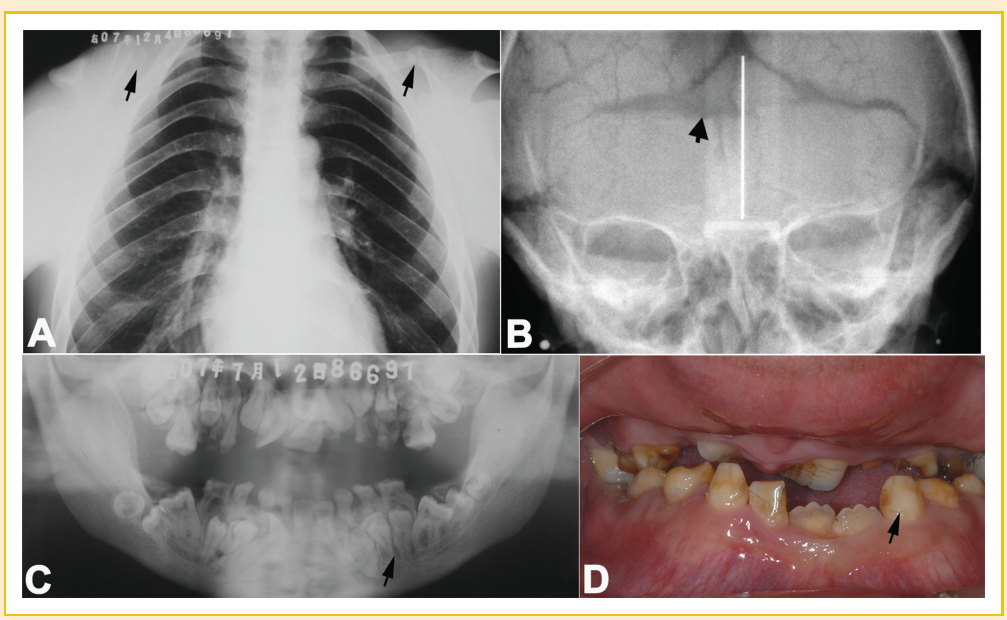

Fig. 2. Clinical and radiological findings of patient 2. A: Chest radiograph showing the same hypoplasia as his sister. B: Posteroanterior cephalometric radiograph showing more severe open sutures and fontanelle. C: Panoramic view showing impacted permanent teeth and retention of deciduous teeth, no supernumerary teeth. D: Intraoral image showing enamel and dentin hypoplasia.

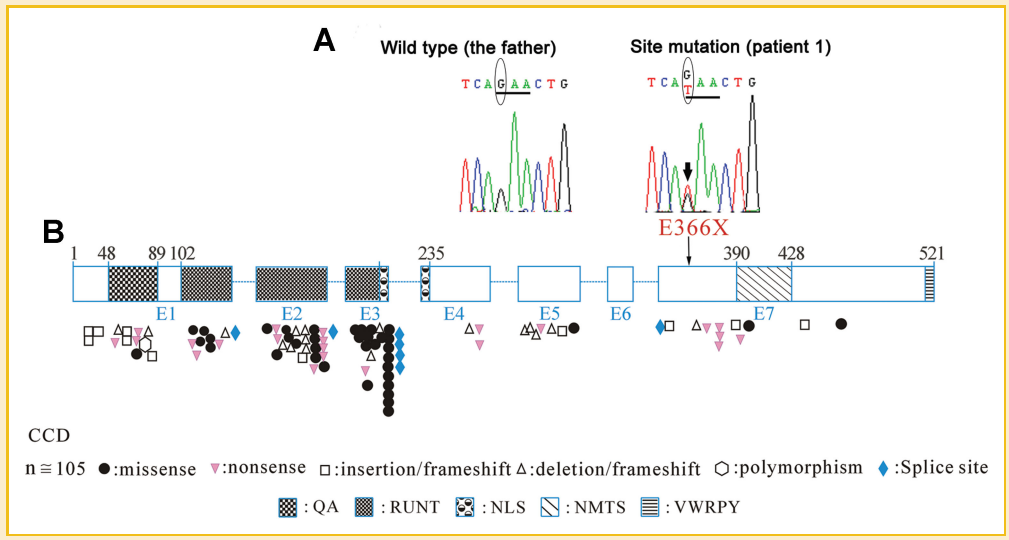

Fig. 3. Mutation analysis of *RUNX2* gene in the CCD patients and the location of mutation sites relative to the structure of the *RUNX2* gene. A: Sequencing results showing the wild-type allele and the heterozygous mutant allele with G > T nonsense mutation. The arrow indicates the mutation site. B: The schematic shows functional domains and the mutation sites of *RUNX2* in CCD patients. Mutations reported in previous studies [Otto et al., 2002; Yoshida et al., 2002; Tessa et al., 2003; Kim et al., 2006; Pal et al., 2007; Xuan et al., 2008; Li et al., 2009; Zhang et al., 2009; Cardoso et al., 2010; Gao et al., 2010; Wang et al., 2010] are indicated below the structure of RUNX2 protein (the 521 amino acids isoform starting with MASNS). The new mutation E366X identified in the present study is indicated above the structure. Symbols used to indicate mutation types are as annotated in the inset.

After we detected that the truncated protein was expressed in $RUNX2^{+/m}$ DPCs and the subcellular localization of RUNX2 was altered, we compared the phenotypic characteristics of DPCs expressing the mutant Runx2 protein with those expressing wild-type RUNX2 protein. Utilizing phase contrast microscopy, $RUNX2^{+/m}$ DPCs appear flatter and larger than $RUNX2^{+/+}$ DPCs (Fig. 5A,B), and the results of the IPE assay indicated that the area size of these cells was significantly different, with the $RUNX2^{+/+}$ cells at $486.58 \pm 93.62\ \mu m^2$, and the $RUNX2^{+/m}$ cells at $874.10 \pm 293.41\ \mu m^2$ ($t = 6.892$, $P = 0.000$).

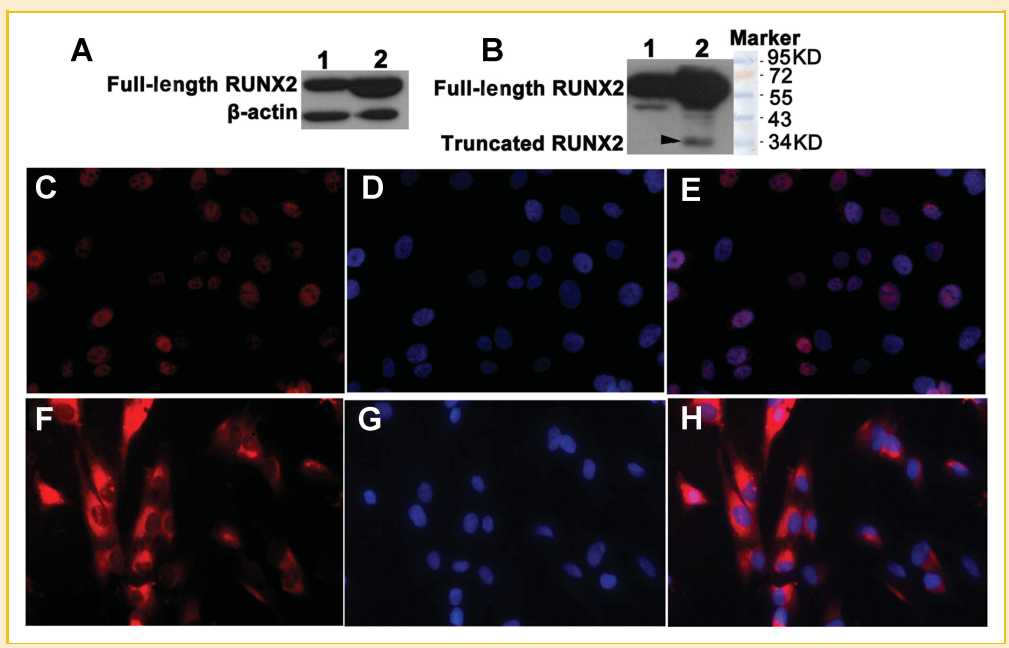

Fig. 4. Expression analysis of RUNX2 protein between $RUNX2^{+/+}$ DPCs and $RUNX2^{+/m}$ DPCs. A and B represent two exposures of Western blotting which showed expression of RUNX2 protein in $RUNX2^{+/+}$ DPCs (line 1) and $RUNX2^{+/m}$ DPCs (line 2). A shows the full-length RUNX2 exposed for 1 min, and β-actin was used as the loading control. B shows that the truncated RUNX2 mutant protein expressed only in $RUNX2^{+/m}$ DPCs (the arrow head indicates), and the exposed time was 30 min. C and D represent nuclear localization of RUNX2 protein in the two group cells, respectively, and almost all the $RUNX2^{+/+}$ cells had the protein localized in the nucleus (C), however, the protein localized mostly in the cytoplasm of the $RUNX2^{+/m}$ DPCs, and a few cells have the protein both in nucleus and the cytoplasm (F). D and G are the corresponding DAPI stainings of C and F, respectively; E is the overlapped pictures of C and D; H is the overlapped pictures of F and G.

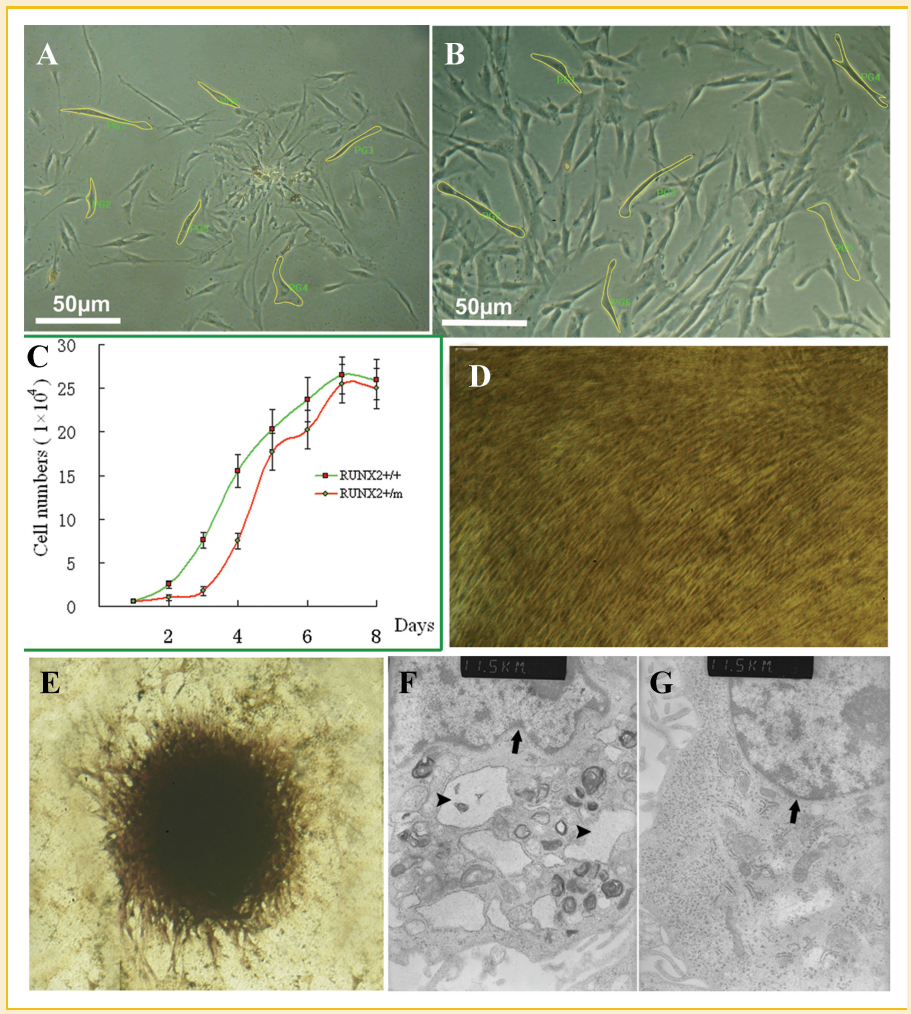

Fig. 5. Comparison of morphology, ultrastructure, growth and differentiation between *RUNX2*$^{+/m}$ and *RUNX2*$^{+/+}$ DPCs. A (100×) (*RUNX2*$^{+/+}$) and B (100×) (*RUNX2*$^{+/m}$) show the morphology and size of the two populations of cells. C shows the growth curve of the two DPCs, and the circle and square represent *RUNX2*$^{+/+}$ and *RUNX2*$^{+/m}$ cells, respectively. The cell numbers were plotted as a graph with the data showing mean ± SE from three independent samples. D and E show the result of von Kossa staining, and calcification nodules were induced in *RUNX2*$^{+/+}$ cells (E), not in *RUNX2*$^{+/m}$ cells (D). F (*RUNX2*$^{+/m}$) and G (*RUNX2*$^{+/+}$) show the ultrastructure of the two populations by EMT; the arrow in the F indicates the irregular nucleus, and the arrowheads indicate the expanded endoplasmic reticulum.

According to the analysis of cell growth, *RUNX2*$^{+/m}$ DPCs presented lower proliferation rate than *RUNX2*$^{+/+}$ cells (Fig. 5C) ($P \leq 0.01$). The results of flow cytometric analysis showed that *RUNX2*$^{+/m}$ DPCs presented significant increase during the G0/G1 phase, with a concomitant decrease in S phase. Furthermore, the proliferation index of the *RUNX2*$^{+/m}$ cells was significantly decreased relative to their wild-type *RUNX2*$^{+/+}$ counterparts (Table II).

During the calcification induction, *RUNX2*$^{+/m}$ cells had never formed mineralized nodules, even when the cells were induced for seven weeks, although some cells exhibited overlapping growth (Fig. 5D). Nonetheless, *RUNX2*$^{+/+}$ DPCs presented condensed mineralized nodules (Fig. 5E).

The ultrastructure of the cells was further examined. Compared with *RUNX2*$^{+/+}$ cells, most of the *RUNX2*$^{+/m}$ cells presented

TABLE II. Flow Cytometric Analysis of Cell Cycle and Proliferation Index (PI) Between *RUNX2*$^{+/-}$ and *RUNX2*$^{+/+}$ DPCs (Means ± SE), PI = (S+G2/M), (G0/G1+S+G2/M) × 100%

	Cell cycle			
	G0/G1 (%)	S (%)	G2 + M (%)	Proliferation index (%)
RUNX2$^{+/+}$ (n = 3)	51.06 ± 3.84	38.4 ± 3.30	10.53 ± 0.72	48.93 ± 2.01
RUNX2$^{+/-}$ (n = 3)	76.70 ± 2.10[a]	14.2 ± 1.70[a]	9.06 ± 0.83	23.26 ± 1.70[a]

[a]Significantly different from the *RUNX2*$^{+/+}$ group ($P < 0.01$).

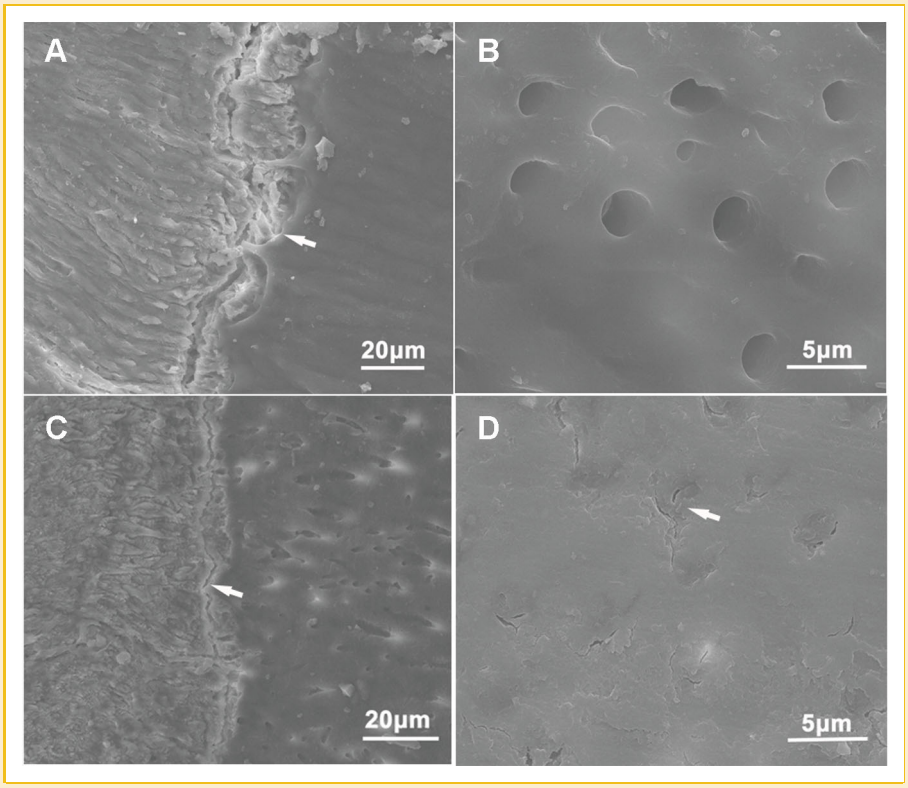

Fig. 6. SEM analysis of tooth from CCD patient 1 and the corresponding normal individual respectively. A (1,000×) and B (5,000×), respectively, presented typical scallop enamel–dentin junction (EDJ) (the arrow indicates) and regularly arranged and clear dentin tubules in normal controls. C (1,000×) and D (5,000×), respectively, presented flatter EDJ (the arrow indicates) and irregular and obliterative dentin tubules (the arrow indicates) in CCD tooth.

irregular nuclei, rough and expanded endoplasmic reticulums, partial ribosome detachment, and many lamellar bodies in the cytoplasm (Fig. 5F,G).

DENTIN OF CCD TEETH PRESENTED POOR MINERALIZATION

To visualize the mineralization of CCD teeth, we examined dentin specimens using SEM and EDS analyses. Compared with normal teeth (Fig. 6A,B), CCD teeth exhibited flatter enamel–dentin junction (EDJ), no typical scallop structure existed, and dentin tubules appeared irregular and obliterative, and peritubular dentin presented obscure and inadequate mineralization (Fig. 6C,D). Compared with that of normal teeth, the dentin of the CCD teeth showed a significant decrease in calcium and phosphonium composition, and carbon and oxygen composition was increased correspondingly (Table III).

DISCUSSION

In the present study, a family with CCD was analyzed, and a novel nonsense mutation (p.E366X) was identified in the two CCD patients. Although a blood sample was not obtained from the mother, she was examined clinically, and did not have any findings suggestive of CCD. Her clavicles were easily palpable, her fontanel closed and she had no dental anomalies. Chest X-ray confirmed presence of normal clavicles. The father was unaffected clinically and genetically. It is inferred that there would be an existence of germ line mosaicism in the CCD family as reported [Pal et al., 2007]. Further testing through heteroduplex analysis needs to be done to provide molecular data.

In the SNP database, 970 SNPs were found within the *homo sapiens RUNX2* gene, and the c. 1096 G > T (p.E366X) site is absent from the database, suggesting that these CCD patients possess a

TABLE III. EDS Analysis of Dentin Elements Between CCD and Normal Tooth (Means ± SE)

	Ca (n = 3) (weight %)	P (n = 3) (weight %)	C (n = 3) (weight %)	O (n = 3) (weight %)
Normal	17.98 ± 0.728	6.57 ± 0.021	52.92 ± 0.692	21.92 ± 0.551
CCD	11.04 ± 0.707[a]	1.93 ± 0.070[a]	59.46 ± 0.834	26.74 ± 0.169
t	9.676	88.982	8.527	11.812
P	0.011	0.003	0.015	0.035

[a]Significantly lower than normal.

novel nonsense heterozygous mutation. Furthermore, in the present study, the E366X nonsense mutation was detected to create a shortened protein product, which was present only in the *RUNX2*$^{+/m}$ DPCs, and localized mostly in the cytoplasm, other than in the nucleus exclusively as the wild RUNX2 protein. According to the putative functional domain of the *RUNX2* gene [Thirunavukkarasu et al., 1998], E366 is located in the third transactivation element 3 (TE3) within the proline/serine/threonine (PST)-rich domain, and most importantly, E366 is within the GASEL motif which is involved in the transactivation function of TE3.

To further assess the effect of the novel truncated protein on tooth development, we investigated the growth and differentiation potential of the *RUNX2*$^{+/m}$ DPCs. Compared to *RUNX2*$^{+/+}$ cells, *RUNX2*$^{+/m}$ cells exhibited flatter and larger, and showed a lower rate of proliferation. Furthermore, the *RUNX2*$^{+/m}$ cells showed an impeded progression from G1 to S phase in the cell cycle. Therefore, this indicates that the truncated E366X RUNX2 protein may affect both the morphology and proliferation of DPCs. Previous studies have shown that isolated DPCs from normal people could be induced to differentiate into odontoblast-like cells and generate dentin-like mineral structures both in vitro and in vivo [About et al., 2000; Batouli et al., 2003]. Pulp cells with the potential to differentiate into odontoblasts are critical for pulp tissue regeneration and the formation of dentin. Our results indicated that *RUNX2*$^{+/m}$ DPCs exhibited diminished calcification potential. The special ultrastructure of *RUNX2*$^{+/m}$ DPCs implied that the ability of synthesis and secretion of proteins might be affected to some extent. The elemental analysis showed that a significant decrease in calcium and phosphonium composition and the dentin of the corresponding teeth presented inadequate mineralization. Taken together, it is inferred the *RUNX2*$^{+/m}$ DPCs with the poor potential of differentiation may be responsible for dentin dysplasia of the CCD teeth.

In this study, the new Runx2 mutation slowed the proliferation of DPCs in vitro by causing cell cycle arrest in G1. Pratap et al. [2003] reported that calvarial cells but not embryonic fibroblasts from *Runx2*$^{-/-}$ and Runx2$^{\Delta C/\Delta C}$ mutant mice exhibited increased cell growth rates as reflected by elevations of DNA synthesis and G1-S phase markers. It seems that the increased cell growth appear to be restricted to the osteogenic lineage. Different mutations of *RUNX2* gene might have different effect on cell growth because of the different level of functional activity of RUNX2 protein.

The RUNX2 C-terminus contains the subnuclear matrix-targeting signal (NMTS, aa 390–427) and activation domain, which are necessary to direct RUNX2 to subnuclear locations, and the nuclear localization contributes to transactivation of RUNX2 and organization with co-regulatory proteins (e.g., Smad 1,2,3,5), which are essential for normal bone formation [Choi et al., 2001; Lian et al., 2006; Javed et al., 2000]. Taken together, nonsense mutations in the RUNX2 C-terminus can cause different levels of reduction in RUNX2 biological activities, which may be related to the typical CCD phenotype. The shortened E366X mutant protein is lacking the C-terminal 155 amino acids, resulting in loss of nuclear localization. And the mutant is predicted to cause many dysfunctions in DNA binding and transactivation. However, the patients in this study did not present severe CCD phenotype as reported by El-Gharbawy et al. [2010]. In the literature, a child with microdeletion (327aa–521aa) of the C-terminal region of RUNX2 presented severe CCD. The mouse model showed that there was a critical gene dosage requirement of functional Runx2 for the formation of bone tissues during embryogenesis, and the reduction of functional Runx2 dosage altered the expression of osteoblast marker genes and delayed cellular differentiation [Lou et al., 2009]. It is inferred that the level of functional activity of RUNX2 would be determined by both the amount of mutant protein and the type of mutation. The E366X nonsense mutation may cause CCD phenotype by inhibiting cell growth and differentiation and reducing functional activity of RUNX2. These mechanisms provide insight into our understanding of the molecular functions of RUNX2, which mediates abnormalities in dental development and the underlying pathogenesis of CCD.

Truncated proteins may be unstable and can be degraded rapidly (Akeson et al., 1989; Hashimoto et al., 1996), therefore, it is difficult to detect them. In our experiment, the truncated protein was detected only by prolonged exposure time. Maybe the exact quantity of the truncated protein was far more than detected. Although Zhang et al. [2000] reported a nonsense mutation CCDαA376 lacking the C-terminal 130 aa, and the truncated mutant RUNX2 protein was expressed by homologous recombination, however, there has never been a truncated RUNX2 protein to be explored in tissues or cells of the CCD patients themselves. In the present study, the novel E366X mutant RUNX2 protein was explored in DPCs isolated from CCD patient 1, and the expression of the mutant protein was examined without effect of any exogenous gene. Therefore, these results could reflect the most natural functional conditions of the RUNX2 protein in CCD patients. Western blotting analysis showed that the level of full-length RUNX2 protein in RUNX2$^{+/m}$ DPCs was no less than that of RUNX2$^{+/+}$ DPCs, however, the subnuclear localization of the majority of RUNX2 protein was excluded from the nucleus by immunocytochemistry analysis, and these indicated that RUNX2 subnuclear targeting might be mostly abrogated. Subnuclear localization of RUNX2 factors and the associated regulatory functions were essential for control of Runx-dependent genes involved in tissue differentiation during embryonic development [Choi et al., 2001]. RUNX2 was regulated, in part, through a negative feedback loop by activity of the RUNX2 protein on its own promoter, to control variations in gene expression and function during osteogenesis [Driss et al., 2000]. For human, the level of RUNX2 functional activity, not dosage itself, may be the critical determinant for the CCD phenotype [Lou et al., 2009]. Taken together, one possibility is that the RUNX2 truncated protein has altered activity of the RUNX2 protein and interactions with coregulatory proteins, which could result in phenotype of CCD patients. Further functional analysis of the RUNX2 truncated protein need to be done to make plain its putative importance in the etiology of CCD.

ACKNOWLEDGMENTS

This work was supported by National Natural Science Foundation of China (grant number: 30901691) and Medical Scientific Research Fund of Guangdong Province (grant number: B2008015).

REFERENCES

Aberg T, Wang XP, Kim JH, Yamashiro T, Bei M, Rice R, Ryoo HM, Thesleff, I. 2004. Runx2 mediates FGF signaling from epithelium to mesenchyme during tooth morphogenesis. Dev Biol 270:76–93.

About I, Bottero MJ, Denato P, Camps J, Franquin JC, Mitsiadis TA. 2000. Human dentin production in vitro. Exp Cell Res 258:33–41.

Akeson AL, Wiginton DA, Hutton JJ. 1989. Normal and mutant adenosine deaminase genes. J Cell Biochem 39:217–228.

Batouli S, Miura M, Brahim J, Tsutsui TW, Fisher LW, Gronthos S, Robey PG, Shi S. 2003. Comparison of stem-cell-mediated osteogenesis and dentinogenesis. J Dent Res 82:976–981.

Cardoso BM, Dupont J, Castanhinha S, Ejarque-Albuquerque M, Pereira S, Miltenberger-Miltenyi G, Oliveira G. 2010. Cleidocranial dysplasia with severe parietal bone dysplasia: A new (p.Val124Serfs) RUNX2 mutation. Clin Dysmorphol 19:150–152.

Chen S, Gu TT, Screenath T, Kulkarni B, MacDougall M. 2002. Spatial expression of Cbfa1/Runx2 isoforms in teeth and characterization of binding sites in the DSPP gene. Connect Tissue Res 43:338–344.

Chen S, Santos I, Wu Y, Vuong R, Gay I, Schulze J, Chuang H, MacDougall M. 2005. Altered gene expression in human cleidocranial dysplasia dental pulp cells. Arch Oral Biol 50:227–236.

Choi JY, Pratap J, Javed A, Zaidi SK, Xing L, Balint E, Dalamangas S, Boyce B, van Wijnen AJ, Lian JB, Stein JL, Jones SN, Stein GS. 2001. Subnuclear targeting of Runx/Cbfa/AML factors is essential for tissue-specific differentiation during embryonic development. Proc Natl Acad Sci 98:8650–8655.

Driss H, Luc Q, Shakoori R, Chuva De Sousa LS, Choi JY, Terry A, Hu M, Jones S, Neil JC, Lian JB, Stein JL, Wunen AJ, Stein GS. 2000. Transcriptional autoregulation of the bone related CBFA1/RUNX2 gene. J Cell Physiol 184:341–350.

D'Souza RN, Aberg T, Gaikwad J, Cavender A, Owen M, Karsenty G. 1999. Cbfa1 is required for epithelial–mesenchymal interactions regulating tooth development in mice. Development 126:2911–2920.

Ducy P, Zhang R, Geoffroy V, Ridall AL, Karsenty G. 1997. Osf2/Cbfa1: A transcriptional activator of osteoblast differentiation. Cell 89:747–754.

El-Gharbawy AH, Peeden JN, Jr., Lachman RS, Graham JM, Jr., Moore SR, Rimoin DL. 2010. Severe cleidocranial dysplasia and hypophosphatasia in a child with microdeletion of the C-terminal region of RUNX2. Am J Med Genet Part A 152A:169–174.

Freshney RI. 2001. Culture of animal cells—A manual of basic technique. New York: Wiley-Liss. pp. 227–244.

Gao C, Wu L, Geng XJ, Song LJ, Luo Q. 2010. Two novel RUNX2 gene mutations in two Chinese families with cleidocranial dysplasia. Zhonghua Yi Xue Yi Chuan Xue Za Zhi 27:140–143.

Goldberg M, Lasfargues JJ. 1995. Pulpo-dentinal complex revisited. J Dent 23:15–20.

Hashimoto S, Tsukada S, Matsushita M, Miyawaki T, Niida Y, Yachie A, Kobayashi S, Iwata T, Hayakawa H, Matsuoka H, Tsuge I, Yamadori T, Kunikata T, Arai S, Yoshizaki K, Taniguchi N, Kishimoto T. 1996. Identification of Bruton's tyrosine kinase (Btk) gene mutations and characterization of the derived proteins in 35 X-linked agammaglobulinemia families: A nationwide study of Btk deficiency in Japan. Blood 88:561–573.

Javed A, Guo B, Hiebert S, Choi J-Y, Green J, Zhao SC, Osborne MA, Stifani S, Stein JL, Lian JB, van Wijnen AJ, Stein GS. 2000. Groucho/TLE/R-esp proteins associate with the nuclear matrix and repress RUNX (CBF(alpha)/AML/PEBP2(alpha)) dependent activation of tissue-specific gene transcription. J Cell Sci 113:2221–2231.

Kim HJ, Nam SH, Kim HJ, Park HS, Ryoo HM, Kim SY, Cho TJ, Kim SG, Bae SC, Kim IS, Stein JL, Van WA, Stein GS, Lian JB, Choi JY. 2006. Four novel RUNX2 mutations including a splice donor site result in the cleidocranial dysplasia phenotype. J Cell Physiol 207:114–122.

Li Y, Pan W, Xu W, He N, Chen X, Liu H, Darryl Quarles L, Zhou H, Xiao Z. 2009. RUNX2 mutations in Chinese patients with cleidocranial dysplasia. Mutagenesis 24:425–431.

Lian JB, Stein GS, Javed A, van Wijnen AJ, Stein JL, Montecino M, Hassan MQ, Gaur T, Lengner CJ, Young DW. 2006. Networks and hubs for the transcriptional control of osteoblastogenesis. Rev Endocr Metab Disord 7:1–16.

Lou Y, Javed A, Hussain S, Colby J, Frederick D, Pratap J, Xie R, Gaur T, van Wijnen AJ, Jones SN, Stein GS, Lian JB, Stein JL. 2009. A Runx2 threshold for the cleidocranial dysplasia phenotype. Hum Mol Genet 18:556–568.

Mundlos S. 1999 Cleidocranial dysplasia: Clinical and molecular genetics. J Med Genet 36:177–182.

Mundlos S, Otto F, Mundlos C, Mulliken JB, Aylsworth AS, Albright S. 1997. Mutations involving the transcription factor CBFA1 gene cause cleidocranial dysplasia. Cell 89:773–779.

Otto F, Kanegane H, Mundlos S. 2002. Mutations in the RUNX2 gene in patients with cleidocranial dysplasia. Human Mutat 19:209–216.

Pal T, Napierala D, Becker TA, Loscalzo M, Baldridge D, Lee B, Sutphen R. 2007. The presence of germ line mosaicism in cleidocranial dysplasia. Clin Genet 71:589–591.

Pratap J, Galindo M, Zaidi SK, Vradii D, Bhat BM, Robinson JA, Choi JY, Komori T, Stein JL, Lian JB, Stein GS, van Wijnen AJ. 2003. Cell growth regulatory role of Runx2 during proliferative expansion of preosteoblasts. Cancer Res 63:5357–5362.

Tessa A, Salvi S, Casali C, Garavelli L, Digilio MC, Dotti MT, Giandomenico SD, Valoppi M, Grieco GS, Comanducci G, Bianchini G, Fortini D, Federico A, Giannotti A, Santorelli FM. 2003. Six novel mutations of the RUNX2 gene in Italian patients with cleidocranial dysplasia. Hum Mutat 22:104.

Thirunavukkarasu K, Magajaan M, Mclarren KW, Stifani S, Karsenty G. 1998. Two domains unique to osteoblast-specific transcription factor Osf2/Cbfa1 contribute to its transactivation function and its inability to heterodimerize with Cbfβ. Mol Cell Biol 18:4197–4208.

Wang GX, Sun RP, Song FL. 2010. A novel RUNX2 mutation (T420I) in Chinese patients with cleidocranial dysplasia. Genet Mol Res 9:41–47.

Xuan DY, Li S, Zhang X, Lin L, Wang C, Zhang J. 2008. A novel RUNX2 mutation in cleidocranial dysplasia patients. Biochem Genet 46:702–707.

Yoshida T, Kanegane H, Osato M, Yanagida M, Miyawaki T, Ito Y, Shigesada K. 2002. Functional analysis of RUNX2 mutations in Japanese cases with cleidocranial dysplasia demonstrates novel genotype-phenotype correlations. Am J Hum Genet 71:724–738.

Zhang YW, Yasui N, Ito K, Huang G, Fujii M, Hanai J, Nogami H, Ochi T, Miyazono K, Ito Y. 2000. A RUNX2/PEBP2alpha A/CBFA1 mutation displaying impaired transactivation and Smad interaction in cleidocranial dysplasia. Proc Natl Acad Sci 97:10549–10554.

Zhang CY, Zheng SG, Wang YX, Zhu JX, Zhu X, Zhao YM, Ge LH. 2009. Novel RUNX2 mutations in Chinese individuals with cleidocranial dysplasia. J Dent Res 88:861–866.